Published in final edited form as:
Ultramicroscopy. 2014 January ; 136: 211–215. doi:10.1016/j.ultramic.2013.10.009.

Combined single cell AFM manipulation and TIRFM for probing the molecular stability of multilayer fibrinogen matrices

W. Christenson[a,b], **I. Yermolenko**[a,c], **B. Plochberger**[a,1], **F. Camacho-Alanis**[d], **A. Ros**[d], **T.P. Ugarova**[c], and **R. Ros**[a,b,*]

[a]Department of Physics, Arizona State University, Tempe, AZ 85287, USA

[b]Center for Biological Physics, Arizona State University, Tempe, AZ 85287, USA

[c]School of Life Sciences, Arizona State University, Tempe, AZ 85287, USA

[d]Department of Chemistry and Biochemistry, Arizona State University, Tempe, AZ 85287, USA

Abstract

Adsorption of fibrinogen on various surfaces produces a nanoscale multilayer matrix, which strongly reduces the adhesion of platelets and leukocytes with implications for hemostasis and blood compatibility of biomaterials. The nonadhesive properties of fibrinogen matrices are based on their extensibility, ensuing the inability to transduce strong mechanical forces via cellular integrins and resulting in weak intracellular signaling. In addition, reduced cell adhesion may arise from the weaker associations between fibrinogen molecules in the superficial layers of the matrix. Such reduced stability would allow integrins to pull fibrinogen molecules out of the matrix with comparable or smaller forces than required to break integrin–fibrinogen bonds. To examine this possibility, we developed a method based on the combination of total internal reflection fluorescence microscopy, single cell manipulation with an atomic force microscope and microcontact printing to study the transfer of fibrinogen molecules out of a matrix onto cells. We calculated the average fluorescence intensities per pixel for wild-type HEK 293 (HEK WT) and HEK 293 cells expressing leukocyte integrin Mac-1 (HEK Mac-1) before and after contact with multilayered matrices of fluorescently labeled fibrinogen. For contact times of 500 s, HEK Mac-1 cells show a median increase of 57% of the fluorescence intensity compared to 6% for HEKWT cells. The results suggest that the integrin Mac-1-fibrinogen interactions are stronger than the intermolecular fibrinogen interactions in the superficial layer of the matrix. The low mechanical stability of the multilayer fibrinogen surface may contribute to the reduced cell adhesive properties of fibrinogen-coated substrates. We anticipate that the described method can be applied to various cell types to examine their integrin-mediated adhesion to the extracellular matrices with a variable protein composition.

*Corresponding author at: Department of Physics, Arizona State University, Tempe, AZ 85287, USA. Tel.: +1 480 727 9280; fax: +1 480 965 7954. Robert.Ros@asu.edu (R. Ros).
[1]Present address: Vienna University of Technology, Institute of Applied Physics-Biophysics, Wiedner Hauptstraße 8-10, 1040 Vienna, Austria.

Keywords

Single cell force spectroscopy; Atomic force microscopy; Total internal reflection fluorescence; microscopy; Cell adhesion; Integrins; Fibrinogen

1. Introduction

Fibrinogen is a multifunctional plasma protein, which plays a central role in hemostasis and wound healing. During blood vessel injury, fibrinogen is converted to a fibrin clot, which seals the breach and prevents blood loss. Fibrinogen also contains binding sites for integrin receptors on platelets and leukocytes. Consequently, in addition to acting as a mechanical scaffold of clots, fibrin(ogen) can serve as an adhesive substrate for blood cells. Besides its role in hemostasis, fibrinogen deposition on implanted biomaterials may affect their biocompatibility by promoting the adhesion of platelets and leukocytes, which, as generally believed, can trigger unwanted processes such as thrombosis and inflammation. We have recently identified a previously unrecognized fibrinogen-dependent mechanism that controls adhesion of blood cells [1–4]. Specifically, we have found that the ability of fibrinogen to support cell adhesion strikingly depends on its coating concentration: while low-density fibrinogen is deposited in a (sub)-monolayer form which is highly adhesive for platelets and leukocytes, its adsorption on various surfaces at high concentrations results in the formation of multilayered matrix incapable of supporting integrin-mediated cell adhesion. In the multilayer, fibrinogen molecules interact with each other through their flexible αC regions [1]. The conversion of a highly adhesive, low-density fibrinogen monolayer to the nonadhesive fibrinogen multilayer occurs within a very narrow range of fibrinogen coating concentrations [1–4]. A molecular basis for the nonadhesive properties of the fibrinogen matrices is their extensibility, ensuing the inability to transduce strong mechanical forces via cellular integrins and resulting in weak intracellular signaling. Reduced cell adhesion may also arise from the weaker associations between fibrinogen molecules in the superficial layers of the matrix leading to reduced stability. The latter would allow integrins to extract fibrinogen molecules from the matrix with comparable or smaller forces than necessary to break integrin–fibrinogen bonds.

Atomic force microscopy (AFM) [5], primarily known as a high resolution imaging technique, can be utilized for precise force measurements with pN resolution [6–11]. In single cell force spectroscopy (SCFS) [2,12–22], AFM is applied to manipulate single living cells and quantify interaction forces between the cells and substrates or other cells. For this technique, a single cell is attached to a tipless AFM cantilever, brought into contact with the surface or another cell, and retracted while the acting force is monitored. AFM can be combined with various optical microscopy techniques like widefield optical epifluorescence and differential interference contrast microscopy [23], total internal reflection fluorescence microscopy (TIRFM) [24–26], two-photon microscopy [27], confocal fluorescence microscopy [28–30], fluorescence lifetime imaging microscopy [29–31], and optical superresolution microscopy techniques [32].

In this paper, we describe a novel method based on the combination of single cell manipulation by an AFM, TIRFM and microcontact printing [33] (Fig. 1a) to study the stability of multilayer fibrinogen matrices and address a question whether weak intermolecular forces in the matrix can play an additional role in the low adhesive properties of such surfaces.

2. Methods

2.1. Combined AFM-TIRFM setup

A MFP-3D AFM (Asylum Research) placed on an inverted microscope (IX71, Olympus) was used in combination with a custom setup for objective-type TIRFM. This setup is part of a combined AFM-confocal fluorescence lifetime microscope [29,30,34]. We used a 100× oil immersion objective with a NA of 1.45 (Olympus) and a 640 nm diode laser (LDH-D-C-640, PicoQuant). The total internal reflection angle was aligned manually. The laser was pulsed at 10 Hz during image sequencing. Image sequences were recorded using an EMCCD camera (Ixon+ DU897, Andor) with 132 ms per frame. The image sequences were analyzed using ImageJ [35]. The average pixel intensity was determined from measuring the intensity of all pixels within a 15 μm diameter circle surrounding the location of the cell.

2.2. Cantilever preparation

The cantilevers were prepared as described in [2]. Briefly, tipless silicon nitride cantilevers (HYDRA, AppNano, Santa Clara, CA) were plasma-cleaned at 29.6 W, 400 mTorr in O_2 gas using a plasma cleaner (PDC-001, Harrick Plasma, Ithaca, NY). Cantilevers were incubated in 2 mM (3-Aminopropyl)triethoxysilane (APTES, Sigma) in chloroform solution. After 40 min at 22 °C, the cantilevers were rinsed with chloroform, followed by ethanol and deionized water. Deionized water was supplied from a Milli-Q Synthesis system (Millipore). Cantilevers were incubated in 1.25 mM Bis(sulfosuccinimidyl) suberate sodium salt (BS^3, Sigma) solution for 30 min and then placed into 0.5 mg/ml concanavalin A (Sigma) solution for 30 min at 22 °C. Cantilevers were then rinsed with phosphate buffered saline (PBS) and stored in 1 M NaCl at 4 °C.

2.3. Sample preparation

Human fibrinogen was obtained from Enzyme Research Laboratories (South Bend, IN). Fibrinogen was labeled with Alexa647 (Invitrogen) fluorescent dye according to the manufacturers specifications with an average final 1:1 degree of labeling according to the Invitrogen protocol. Aliquots of labeled protein were stored at −20 °C. Glass bottom petri dishes (Fluorodish FD-5040, World Precision Instruments) were patterned using microcontact printing where a PDMS stamp was placed on the glass surface creating a temporary microfluidic network [36]. The inverted microstructure was created on a Si wafer via photolithography as previously reported [37,38]. Briefly, a Si wafer was spin-coated with the negative photoresist SU-8, UV-exposed through a chrome on soda-lime photomask (Photosciences), and developed in a developer bath. This structure served as the master wafer for elastomer molding. The latter step was performed by casting PDMS on the master wafer and curing for 4 h at 65 °C. Subsequently, the structured PDMS slab was peeled off from the wafer. In total, 100 μL of 100 μg/mL fibrinogen solution was drawn into the

microfluidic network via vacuum and allowed to incubate for 1 h. Excess fibrinogen was removed by flowing 300 μL of PBS through the temporary microfluidic network. Upon removal of the stamp, 2 mL of PBS containing 1% bovine serum albumin (BSA) was allowed to incubate on the surface. BSAwas selected as a commonly used nonadhesive substrate for integrin-bearing cells. The BSA solution was rinsed away and replaced with Hank's balanced salt solution (HBSS) containing Ca^{2+} and Mg^{2+} and 0.1% BSA.

2.4. Cell culture

Human embryonic kidney 293 cells (HEK 293) stably expressing leukocyte integrin $\alpha_M\beta_2$ (aka Mac-1) have been described previously [39,40]. The $\alpha_M\beta_2$-expressing HEK 293 cells (HEK Mac-1) and their wild-type counterparts (HEK WT) were maintained in Dulbecco's Modified Eagle's medium (DMEM) cell growth media with 10% FBS, 100 IU/mL penicillin, and 100 μg/mL streptomycin at 37 °C. Prior to experiments, cells were detached from the flask with cell dissociation buffer (Cellgro, Mediatech Inc., Manassas, VA), washed in HBSS, and suspended in HBSS with 0.1% BSA.

3. Results and discussions

For our experiments, glass surfaces were functionalized with human fibrinogen labeled with Alexa647 and BSA in a defined pattern using a temporary microfluidic network (MFN) in which the fibrinogen solution was drawn into at 100 μg/ml, a concentration known to produce nonadhesive multilayer matrices [2,3]. Upon removal of the stamp, the remaining surface was coated with BSA to prevent nonspecific binding of cells. This process generates well-defined micrometer fibrinogen/BSA patterned surfaces. Fig. 1b shows a fluorescence microscopy image of such a patterned surface. The brighter stripes are areas covered with the labeled fibrinogen, while in the dark stripes the glass surface is covered with unlabeled BSA. The PDMS stamp was designed to create 20 stripes, each 100 μm wide, of labeled fibrinogen with a section of contrasting BSA 100 μm wide between each stripe.

This patterned surface was used for single cell measurements. A typical measurement sequence is shown in Fig. 1c. First, HEK 293 Mac-1 cells stably expressing the leukocyte integrin $\alpha_M\beta_2$ or HEK 293 WT cells as control were pipetted onto the surface and maintained at 37 °C in HBSS. Then a single cell on the BSA coated region of the surface was selected and picked up by pressing the concanavalin A functionalized AFM cantilever with a contact force of ~500 pN for ~5–30 s on the cell. After the retraction of the cantilever, the cell was allowed to firmly attach to the cantilever. Since this cell was not in contact with an adhesive substrate this assured that no integrin-mediated outside-in signaling occurred. Fig. 1d shows a bright field microscopy image of a single cell attached to an AFM cantilever.

Next, to reduce background we photo-bleached an area in the BSA region using a 640 nm diode laser with maximum intensity for 10 s. On this spot, the previously selected cell was pressed down with a contact force of 500 pN and the fluorescence signal of the cell was imaged in the TIRFM mode for 10 s with a 10 times attenuated laser intensity. The fluorescence intensity recorded in this step is used as reference intensity. The cell was then lifted from the BSA coated substrate and transferred to a fibrinogen region on the sample

surface and pressed down with a contact force of 500 pN remaining on the surface for 500 s. Finally, the cell was lifted again, and moved back to the BSA region.

Fig. 2 shows the retracting parts of force–distance curves of HEK Mac-1 and HEK WT cells after the contact with the fibrinogen multilayer matrices. The observed adhesion forces of both cell types are in good agreement with our previous study [2]. Fig. 2a shows the force–distance curve of a HEK Mac-1 cell with an adhesion force of about 360 pN, while the control measurement with the HEK WT cells shows a lower adhesion force of about 90 pN (Fig. 2b). In our previous study [2], we systematically quantified the adhesion forces of the two cell types under a variation of conditions and substrates. For HEK Mac-1 cells on multilayer matrices (coating concentrations of 2 and 20 μg/mL) we found adhesion forces of 200–400 pN for contact times between 10 and 120 s.

Before the cell was lowered to the BSA region with the same contact force, the area below the cell was photo-bleached for 10 s with maximum laser intensity. The time between when the cell was lifted from the fibrinogen and then lowered onto the BSA after photo-bleaching was less than 60 s.

Fig. 3a shows a TIRFM image of a HEK Mac-1 cell before the contact with a fibrinogen matrix. A low fluorescence background at the position of the cell is visible. After the contact, the fluorescence intensity is increased, indicating that fluorescently labeled fibrinogen molecules were removed from the fibrinogen matrix and attached to the cell (Fig. 3b). As control, the same experimental procedure was performed with HEK WT cells. In Fig. 3c and d, TIRFM images of a HEK WT cell before and after the contact with the fibrinogen matrix are shown. Here, the fluorescence intensity in both images is very similar indicating no significant transfer of fluorescently labeled fibrinogen molecules.

For quantification, we calculated the average fluorescence intensities per pixel for 14 HEK Mac-1 and 18 HEK WT cells before and after the contact with multilayered matrices. The first image captured during image sequencing was used for quantification of average fluorescent intensities per pixel before and after contact with fibrinogen. The fluorescent intensities of all pixels within a 15 μm diameter circle surrounding the cell were averaged. Fig. 4 shows box plots for the relative increase in the average fluorescence intensity per pixel before and after the contact of the cells with the matrices. For the HEK Mac-1 cells, the median of the relative increase is 57%, the 25th percentile is 14%, and the 75th percentile is 93%. For HEK WT cells, the median is 6%, 25th percentile is 2%, and 75th percentile was 19%. The results suggest that integrin $\alpha_M\beta_2$–fibrinogen interactions are stronger than the intermolecular fibrinogen interactions in the superficial layer of the matrix. The low mechanical stability of the multilayer fibrinogen surface may contribute to the reduced cell adhesive properties of fibrinogen-coated substrates.

4. Conclusions

We developed a sensitive single cell method to study the transfer of molecules from a surface to a cell during the detachment process. We found that $\alpha_M\beta_2$ integrins are able to pull fibrinogen molecules out of multilayered matrices. The interaction forces between

fibrinogen molecules in multilayer matrices are smaller or comparable with integrin–fibrinogen interactions suggesting a low mechanical stability of the matrices. This indicates that together with the well accepted increased extensibility of the fibrinogen multilayer the low stability of its surface plays a role in the reduced cell adhesive properties of the fibrinogen matrices. We anticipate that the method described in this paper can be applied to other cell types to examine their integrin-mediated adhesion to extracellular matrices with a variable protein composition. Further, our approach may be used advantageously in defining the activation state of the cell before the experiment and precisely controlling activation times, which is of general interest for all single cell force spectroscopy experiments.

Acknowledgments

This work was supported by NIH R01 HL107539. BP is a recipient of the mobility grant of the GEN-AU project of the Austrian Federal Ministry for Science and Research. WC was supported by GAANN (P200A090123).

References

1. Yermolenko IS, Gorkun OV, Fuhrmann A, Podolnikova NP, Lishko VK, Oshkadyerov SP, Lord ST, Ros R, Ugarova TP. The assembly of nonadhesive fibrinogen matrices depends on the alpha C regions of the fibrinogen molecule. J. Biol. Chem. 2012; 287:41979–41990. [PubMed: 23086938]
2. Yermolenko IS, Fuhrmann A, Magonov SN, Lishko VK, Oshkadyerov SP, Ros R, Ugarova TP. Origin of the nonadhesive properties of fibrinogen matrices probed by force spectroscopy. Langmuir. 2010; 26:17269–17277. [PubMed: 20883009]
3. Podolnikova NP, Yermolenko IS, Fuhrmann A, Lishko VK, Bowen B, Enderlein J, Podolnikov AV, Ros R, Ugarova TP. Control of integrin alpha (IIb)beta(3) outside-in signaling and platelet adhesion by sensing the physical properties of fibrin(ogen) substrates. Biochemistry. 2010; 49:68–77. [PubMed: 19929007]
4. Lishko VK, Burke T, Ugarova T. Antiadhesive effect of fibrinogen: a safeguard for thrombus stability. Blood. 2007; 109:1541–1549. [PubMed: 16849640]
5. Binnig G, Quate CF, Gerber C. Atomic force microscope. Phys. Rev. Lett. 1986; 56:930–933. [PubMed: 10033323]
6. Zlatanova J, Lindsay SM, Leuba SH. Single molecule force spectroscopy in biology using the atomic force microscope. Prog. Biophys. Mol. Biol. 2000; 74:37–61. [PubMed: 11106806]
7. Butt HJ, Cappella B, Kappl M. Force measurements with the atomic force microscope: techniques, interpretation and applications. Surf. Sci. Rep. 2005; 59:1–152.
8. Hinterdorfer P, Dufrene YF. Detection and localization of single molecular recognition events using atomic force microscopy. Nat. Meth. 2006; 3:347–355.
9. Helenius J, Heisenberg CP, Gaub HE, Muller DJ. Single-cell force spectroscopy. J. Cell Sci. 2008; 121:1785–1791. [PubMed: 18492792]
10. Liang J, Fernandez JM. Mechanochemistry: one bond at a time. ACS Nano. 2009; 3:1628–1645. [PubMed: 19572737]
11. Fuhrmann A, Ros R. Single molecule force spectroscopy: a method for quantitative analysis of ligand–receptor interactions. Nanomedicine. 2010; 5:657–666. [PubMed: 20528459]
12. Benoit M, Gabriel D, Gerisch G, Gaub HE. Discrete interactions in cell adhesion measured by single-molecule force spectroscopy. Nat. Cell Biol. 2000; 2:313–317. [PubMed: 10854320]
13. Grandbois M, Dettmann W, Benoit M, Gaub HE. Affinity imaging of red blood cells using an atomic force microscope. J. Histochem. Cytochem. 2000; 48:719–724. [PubMed: 10769056]
14. Benoit M, Gaub HE. Measuring cell adhesion forces with the atomic force microscope at the molecular level. Cells Tissues Organs. 2002; 172:174–189. [PubMed: 12476047]
15. Taubenberger A, Cisneros DA, Friedrichs J, Puech P-H, Muller DJ, Franz CM. Revealing early steps of alpha(2)beta(1) integrin-mediated adhesion to collagen type I by using single-cell force spectroscopy. Mol. Biol. Cell. 2007; 18:1634–1644. [PubMed: 17314408]

16. Helenius J, Heisenberg C-P, Gaub HE, Muller DJ. Single-cell force spectroscopy. J. Cell Sci. 2008; 121:1785–1791. [PubMed: 18492792]

17. Beckmann J, Schubert R, Chiquet-Ehrismann R, Muller DJ. Deciphering Teneurin Domains That Facilitate Cellular Recognition, Cell-Cell Adhesion, and Neurite Outgrowth Using Atomic Force Microscopy-Based Single-Cell Force Spectroscopy. Nano Lett. 2013; 13:2937–2946. [PubMed: 23688238]

18. Boettiger D, Wehrle-Haller B. Integrin and glycocalyx mediated contributions to cell adhesion identified by single cell force spectroscopy. J. Phys.-Condens. Matter. 2010; 22

19. Friedrichs J, Helenius J, Muller DJ. Quantifying cellular adhesion to extracellular matrix components by single-cell force spectroscopy. Nat. Protoc. 2010; 5:1353–1361. [PubMed: 20595963]

20. Dao L, Weiland U, Hauser M, Nazarenko I, Kalt H, Bastmeyer M, Franz CM. Revealing non-genetic adhesive variations in clonal populations by comparative single-cell force spectroscopy. Exp. Cell Res. 2012; 318:2155–2167. [PubMed: 22750102]

21. Elter P, Weihe T, Buehler S, Gimsa J, Beck U. Low fibronectin concentration overcompensates for reduced initial fibroblasts adhesion to a nanoscale topography: single-cell force spectroscopy. Colloids Surf. B-Biointerfaces. 2012; 95:82–89. [PubMed: 22429785]

22. Aliuos P, Fadeeva E, Badar M, Winkel A, Mueller PP, Warnecke A, Chichkov B, Lenarz T, Reich U, Reuter G. Evaluation of single-cell force spectroscopy and fluorescence microscopy to determine cell interactions with femtosecond-laser microstructured titanium surfaces. J. Biomed. Mater. Res. A. 2013; 101A:981–990. [PubMed: 22965938]

23. Madl J, Rhode S, Stangl H, Stockinger H, Hinterdorfer P, Schuetz GJ, Kada G. A combined optical and atomic force microscope for live cell investigations. Ultramicroscopy. 2006; 106:645–651. [PubMed: 16677764]

24. Gumpp H, Stahl SW, Strackharn M, Puchner EM, Gaub HE. Ultrastable combined atomic force and total internal fluorescence microscope. Rev. Sci. Instrum. 2009; 80

25. Oreopoulos J, Yip CM. Probing membrane order and topography in supported lipid bilayers by combined polarized total internal reflection fluorescence-atomic force microscopy. Biophys. J. 2009; 96:1970–1984. [PubMed: 19254557]

26. Kufer SK, Strackharn M, Stahl SW, Gumpp H, Puchner EM, Gaub HE. Optically monitoring the mechanical assembly of single molecules. Nat. Nanotechnol. 2009; 4:45–49. [PubMed: 19119282]

27. Gradinaru CC, Martinsson P, Aartsma TJ, Schmidt T. Simultaneous atomic-force and two-photon fluorescence imaging of biological specimens in vivo. Ultramicroscopy. 2004; 99:235–245. [PubMed: 15149718]

28. Noy A, Huser TR. Combined force and photonic probe microscope with single, molecule sensitivity. Rev. Sci. Instrum. 2003; 74:1217–1221.

29. Fuhrmann A, Staunton JR, Nandakumar V, Banyai N, Davies P, Ros R. AFM stiffness nanotomography of normal, metaplastic and dysplastic human esophageal cells. Phys. Biol. 2011; 8:015007. [PubMed: 21301067]

30. Schulz O, Zhao Z, Ward A, Koenig M, Koberling F, Liu Y, Enderlein J, Yan H, Ros R. Tip induced fluorescence quenching for nanometer optical and topographical resolution. Opt. Nanoscopy. 2013; 2:1.

31. Hu DH, Micic M, Klymyshyn N, Suh YD, Lu HP. Correlated topographic and spectroscopic imaging by combined atomic force microscopy and optical microscopy. J. Lumin. 2004; 107:4–12.

32. Harke B, Chacko JV, Haschke H, Canale C, Diaspro A. A novel nanoscopic tool by combining AFM with STED microscopy. Opt. Nanoscopy. 2012; 1:3.

33. Kumar A, Whitesides GM. Features of gold having micrometer to centimeter dimensions can be formed through a combination of stamping with an elastomeric stamp and an alkanethiol ink followed by chemical etching. Appl. Phys. Lett. 1993; 63:2002–2004.

34. Schulz O, Koberling F, Walters D, Koenig M, Viani J, Ros R. Simultaneous single molecule atomic force and fluorescence lifetime imaging. Proc. SPIE. 2010; 7571:757109.

35. Rasband, WS. ImageJ. Bethesda, Maryland, USA: U.S. National Institutes of Health; 1997–2012. <http://imagej.nih.gov/ij/>

36. Delamarche E, Bernard A, Schmid H, Michel B, Biebuyck HA. Patterned delivery of immunoglobulins to surfaces using microfluidic networks. Science. 1997; 276:779–781. [PubMed: 9115199]

37. Duong TT, Kim G, Ros R, Streek M, Schmid F, Brugger J, Anselmetti D, Ros A. Size dependent free solution DNA electrophoresis in structured micro fluidic systems. Microelectron. Eng. 2003; 67C–68C:905–912.

38. Nakano A, Camacho-Alanis F, Chao T-C, Ros A. Immunoglobulin G and bovine serum albumin streaming dielectrophoresis in a microfluidic device. Electrophoresis. 2011; 32:2314–2322. [PubMed: 21792990]

39. Yakubenko VP, Lishko VK, Lam SCT, Ugarova TP. A molecular basis for integrin alpha(M)beta(2) ligand binding promiscuity. J. Biol. Chem. 2002; 277:48635–48642. [PubMed: 12377763]

40. Lishko VK, Yakubenko VP, Ugarova T. The interplay between integrins alpha (M)beta(2) and alpha(5)beta(1) during cell migration to fibronectin. Exp. Cell Res. 2003; 283:116–126. [PubMed: 12565824]

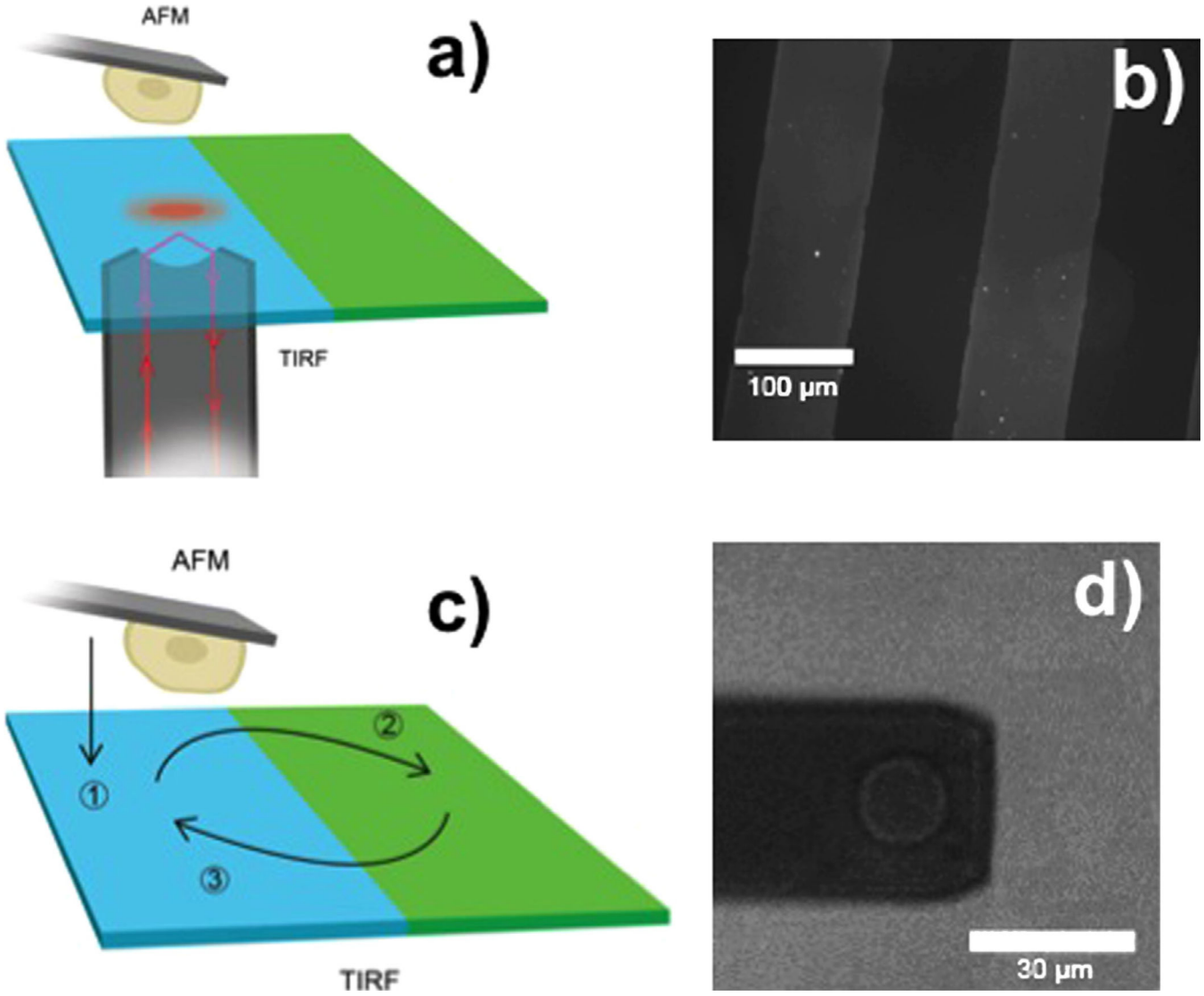

Fig. 1.

(a) Illustration of the experimental setup. A living cell is attached to a tipless AFM cantilever and imaged using TIRFM. The surface contains separated regions with multilayer fibrinogen matrices and BSA. (b) Fluorescence microscopy image of a micro patterned surface. Alexa647 labeled fibrinogen stripes are patterned onto the surface with contrasting unlabeled BSA stripes using microcontact printing methods. (c) Schematic of experimental procedure. A cell is lowered to a surface area covered with unlabeled BSA and imaged with TIRFM (1), the cell is then moved to a surface covered with labeled fibrinogen, and allowed to adhere for 500 s (2), the cell is then transferred back to the unlabeled region, and the fluorescence intensity is measured with TIRFM again (3). (d) Bright field microscopy image of a cell attached to a tipless AFM cantilever.

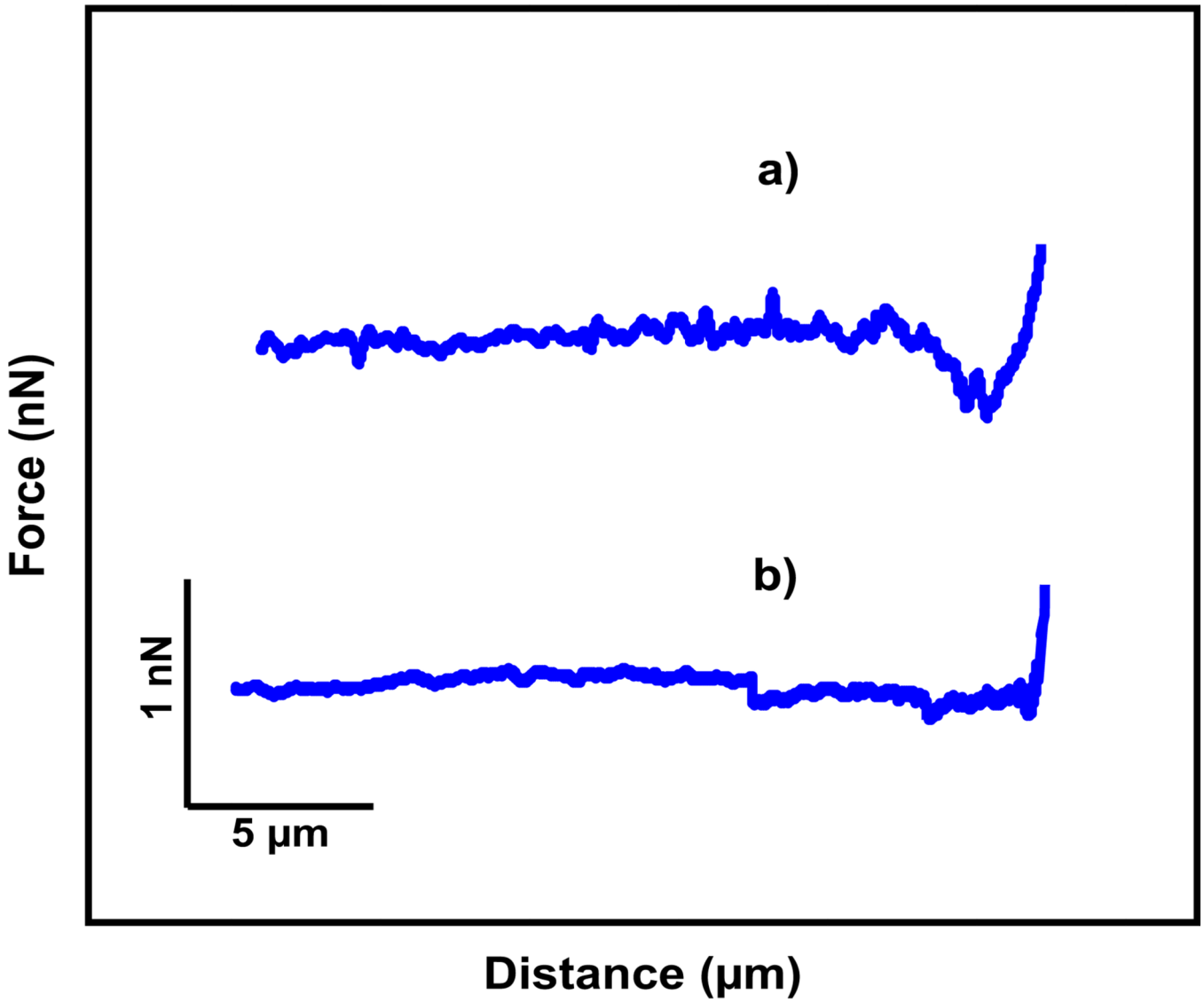

Fig. 2.

Retraction part of force–distance curves after the cell was in contact with the fibrinogen surface. (a) HEK Mac-1 cell is attached to the AFM cantilever and (b) HEK WT cell.

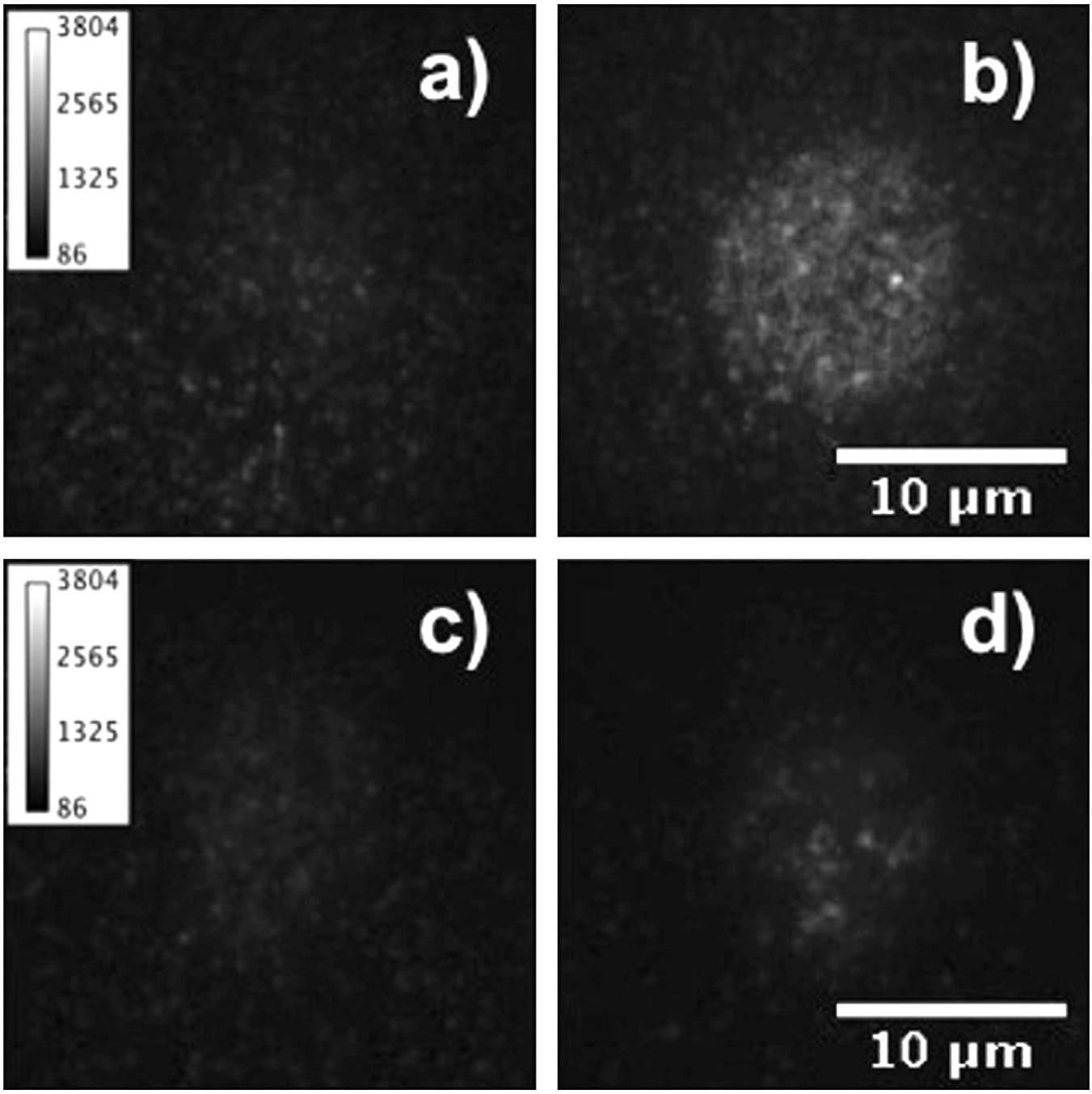

Fig. 3.

TIRFM images of cells before (a and c) and after (b and d) contact with a matrix of fluorescently labeled fibrinogen. In (a) and (b) HEK Mac-1 cell, and in (c) and (d) HEK WT cells are shown. The HEK Mac-1 cell shows a considerable increase in fluorescence intensity after contact with a fibrinogen coated surface.

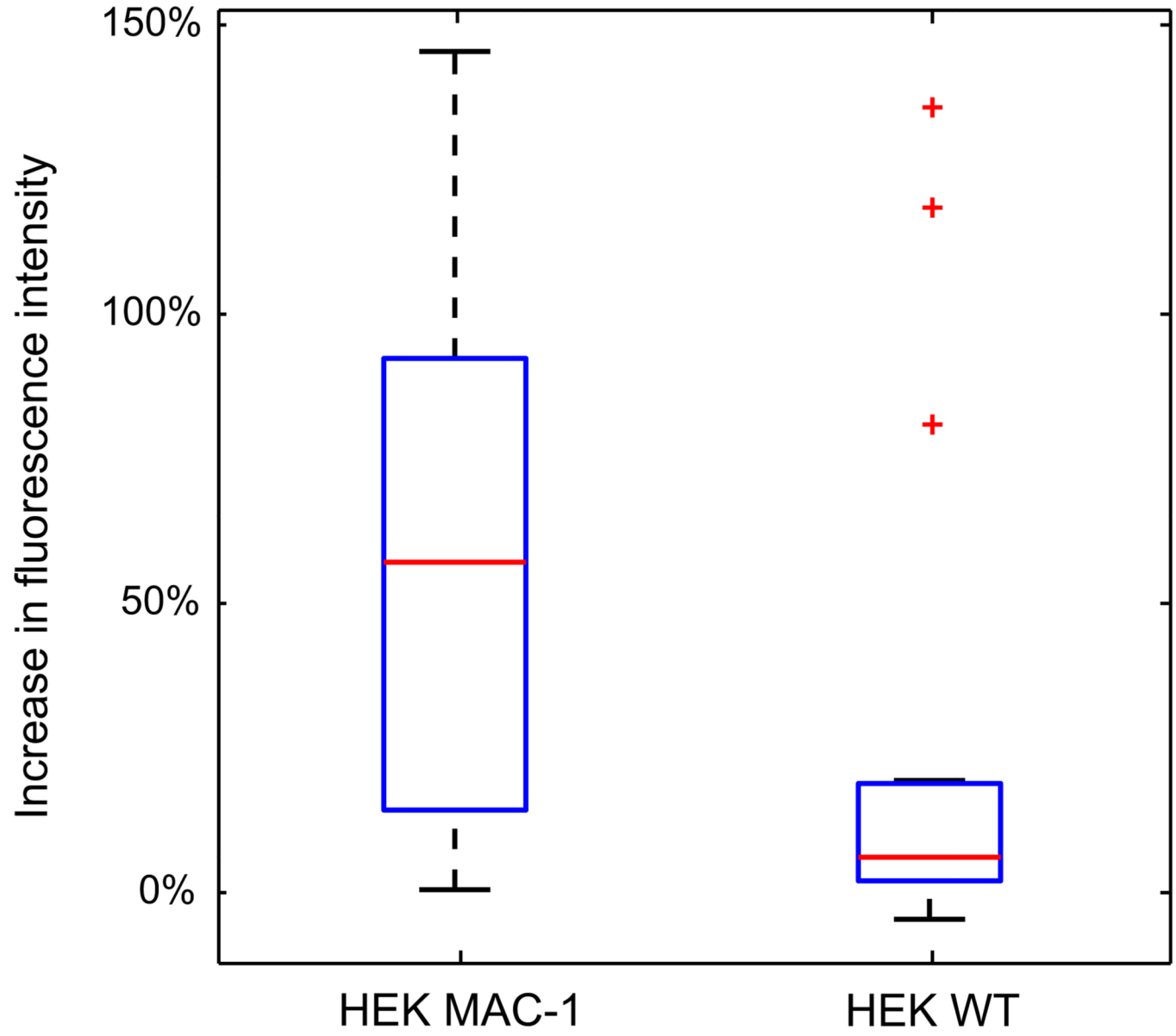

Fig. 4.

Box plot of the relative increase in average fluorescent intensity per pixel of 14 HEK Mac-1 cells and 18 HEK WT cells. The red line represents the median of the data set, and the top and bottom of the box represent the 75th and 25th percentile. For the HEK Mac-1 cells the median is 56.8%, the 25th percentile is 14.2%, and the 75th percentile is 92.6%. For HEK WT cells the median is 6.1%, 25th percentile is 2.0%, and 75th percentile is 18.8%. (For interpretation of the references to color in this figure legend, the reader is referred to the web version of this article.)